Adaptive Fuzzy Observer-Based Command Filtered Discrete-Time Control for PMSMs With Input Constraint

YUMENG XU, JIAPENG LIU, QIXIN LEI, YUMEI MA, AND JINPENG YU

College of Automation, Qingdao University, Qingdao 266071, China
Shandong Key Laboratory of Industrial Control Technology, Qingdao 266071, China

Corresponding author: Jinpeng Yu (yjp1109@hotmail.com)

ABSTRACT This paper proposes an adaptive fuzzy observer-based command filtered discrete-time control method for permanent magnet synchronous motors (PMSMs) with input constraint. First, the rotor angular velocity is estimated by using an adaptive fuzzy observer and the unknown nonlinear function is approximated by using fuzzy logic systems (FLSs) in the PMSMs drive systems. Then, compared with the traditional backstepping method, command filtered backstepping method is developed to solve the "complexity of computation" problem. It is shown that all signals of the closed-loop system are semi-globally uniformly ultimately bounded. Finally, the results of the simulation and experiment demonstrate that the new design method can fully consider the influence of input constraint and load disturbance, and improve the tracking performance for PMSMs drive systems.

INDEX TERMS Command filtered backstepping, adaptive fuzzy observer, input constraint, discrete-time, permanent magnet synchronous motors.

I. INTRODUCTION

In recent years, PMSMs have played a vital role in industrial and agricultural production and have occupied an important position due to meaningful characteristics, such as simple structure, convenient maintenance and reliable operation [1]. In practice, PMSMs drive systems are highly nonlinear, strongly coupled and undetermined parameters in character, which reduce system performance and control accuracy [2]. It can be observed that good control performance is affected by an unknown load disturbance which makes the design of the controller becomes more complicated [3]. For the above cases, it is essential to find a good control method to highlight the advantages of the PMSMs drive systems. In the last decade, relevant scholars have put forward various control methods, such as backstepping control [4]–[8], sliding

mode control [9]–[12], adaptive control [13]–[16], command filtered control (CFC) [17]–[19], fuzzy control and so on.

Nevertheless, it is notable that the above control methods have not explicitly taken input constraint into account on PMSMs drive systems. In practical engineering field, input saturation is inevitable, which will reduce the control accuracy of the system [20]. The sudden increase in voltage will damage the PMSMs drive systems and affect the normal use of the PMSMs in acute cases. A bounded saturation function was used to solve the input saturation problem [21]–[23]. In [24], [25], the function approximation method was proposed to compensate actuator saturation nonlinearity. The anti winding mechanism or auxiliary mechanism was shown to solve the input constraint problem in [26]–[28]. Therefore, fully considering the effect of input saturation is still a huge challenge in the process of controller design. However, [20]–[28] were built on continuous-time conditions and cannot be accurately reflected in the field of digital computers. Generally, digital computer has the characteristics

of fast operation speed and strong anti-interference ability, which is widely used in discrete-time system [29], [30]. The digital computer as a controller, discrete-time system has more advantages than continuous-time system in stability and realizability. It is worth noting that considering the influence of input constraint is still a challenging task for PMSMs discrete-time system.

In another research field, backstepping method [31] is an advanced control method which is widely used in the control field. Unfortunately, in the process of calculating the difference of virtual control function, the "complexity of computation" problem will produce. For the "complexity of computation" problem, dynamic surface control (DSC) technique was investigated in [32]–[34]. DSC method uses the first-order filters to obtain the information of the future state and the difference problem of the virtual control function is solved. However, the errors of first-order filters is generated in DSC technology, which increases the complexity of the algorithm and reduces the control accuracy of the system. Guided by the above methods, [35], [36] proposed CFC method and introduced compensation signal to eliminate filtering errors. In [37], the command filter was designed based on the backstepping method to solve the problem of repeated derivation. The above method is that the state of the system can be measured. References [31]–[37] will inevitably produce some shortcomings when using physical sensor in actual engineering applications, such as cost of the system increases, the reliability decreases and the performance degradation by vibration. It is worth noting that the rotor angular velocity is estimated through a reduced-order observer, which has the characteristics of simple structure and low dimensionality in [38]–[40]. As far as we know, the combination of reduced-order observer and CFC method is not fully considered in the PMSMs drive systems.

In view of the above analysis results, an adaptive fuzzy observer based on command filtered discrete-time control method is proposed for input constraints in this paper. The input constraint and unknown load disturbance are fully considered in the controller design. Specifically, the main benefits of the controller design in this paper are as follows:

- Compared with DSC method [32]–[34], the CFC method solves the "complexity of computation" of the traditional backstepping method and eliminates the problem of filter errors by introducing compensation mechanism.
- The rotor angular velocity is estimated by the designed reduced-order observer. There is no need to directly measure the state of the system, reducing the complexity of the hardware and improving the reliability of the motor.
- Considering the input constraints and load disturbance, the stability of PMSMs drive system is improved, which is more conducive to practical application.

II. REDUCED-ORDER OBSERVER-BASED DISCRETE-TIME MODEL WITH INPUT CONSTRAINT

The discrete-time system model of PMSMs is described as [6]:

$$
\begin{cases}
\theta(k+1) = \Delta_T \omega(k) + \theta(k), \\
\omega(k+1) = \omega(k) + \Delta_T \dfrac{3n_p\phi}{2J} i_{qs}(k) - \Delta_T \dfrac{B}{J}\omega(k) \\
+ \dfrac{3n_p(l_d - l_q)i_{ds}(k)i_{qs}(k)\Delta_T}{2J} - \dfrac{T_l\Delta_T}{J}, \\
i_{qs}(k+1) = -\dfrac{R_s i_{qs}(k)\Delta_T}{l_q} - \dfrac{n_p\phi\omega(k)\Delta_T}{l_q} + \dfrac{u_{qs}(k)\Delta_T}{l_q} \\
- \dfrac{n_p l_d \omega(k) i_{ds}(k)\Delta_T}{l_q} + i_{qs}(k), \\
i_{ds}(k+1) = i_{ds}(k) - \dfrac{R_s i_{ds}(k)\Delta_T}{l_d} + \dfrac{n_p l_q \omega(k) i_{qs}(k)\Delta_T}{l_d} \\
+ \dfrac{u_{ds}(k)\Delta_T}{l_d}.
\end{cases}
$$

The physical meaning of symbols is listed in Table 1.

TABLE 1. Defining symbols.

Symbol	Physical meaning	Unit
ϕ	the magnetic flux	Wb
ω	the rotor angular velocity	rad/s
θ	the rotor position	rad
T_l	the load torque	N $\cdot$ m
J	the rotor inertia	Kg $\cdot$ m^2
B	the coefficient of friction	N $\cdot$ m/(rad/s)
Δ_T	the sampling period	s
n_p	the pole number	/
R_s	the resistance of stator	Ω
l_d and l_q	the q and d axis mutual inductance	H
u_{qs} and u_{ds}	the q and d axis voltages	V
i_{qs} and i_{ds}	the q and d axis currents	A

For the convenience of calculation, the following system variables are introduced and defined as:

$$\psi_1(k) = \theta(k),\ \psi_2(k) = \omega(k),\ \psi_3(k) = i_{qs}(k),$$

$$\psi_4(k) = i_{ds}(k),\ a_1 = \frac{3n_p\phi}{2J},\ a_2 = -\frac{B}{J},$$

$$a_3 = \frac{3n_p(l_d - l_q)}{2J},\ a_4 = -\frac{1}{J},\ b_1 = -\frac{R_s}{l_q},\ b_2 = -\frac{n_p\phi}{l_q},$$

$$b_3 = -\frac{n_p l_d}{l_q},\ b_4 = \frac{1}{l_q},\ c_1 = -\frac{R_s}{l_d},\ c_2 = \frac{n_p l_q}{l_d},\ c_3 = \frac{1}{l_d}.$$

$$(1)$$

Then according to the above notations, the dynamic mathematical model of PMSMs can be transformed into:

$$
\begin{cases}
\psi_1(k+1) = \psi_1(k) + \Delta_T \psi_2(k), \\
\psi_2(k+1) = a_1\Delta_T \psi_3(k) + (1 + a_2\Delta_T)\psi_2(k) \\
+ a_3\Delta_T \psi_3(k)\psi_4(k) + a_4\Delta_T T_l, \\
\psi_3(k+1) = (1 + b_1\Delta_T)\psi_3(k) + b_2\Delta_T \psi_2(k) \\
+ b_3\Delta_T \psi_2(k)\psi_4(k) + b_4\Delta_T u_{qs}(k), \\
\psi_4(k+1) = (1 + c_1\Delta_T)\psi_4(k) + c_3\Delta_T u_{ds}(k) \\
+ c_2\Delta_T \psi_2(k)\psi_3(k).
\end{cases}
\quad (2)
$$

For discrete-time model of the PMSMs drive systems (2), the purpose of designing controller $u_{qs}(k)$ and $u_{ds}(k)$ in this paper is to ensure that the rotor position $\psi_1(k)$ quickly track a given signal $\psi_{1d}(k)$.

Lemma 1 [36]: For discrete-time systems, command filter is defined as:

$$c_{i,1}(k+1) = c_{i,1}(k) + \Delta_T \omega_n c_{i,2}(k),$$
$$c_{i,2}(k+1) = c_{i,2}(k) + \Delta_T[-2\zeta\omega_n c_{i,2}(k) - \omega_n(c_{i,1}(k) - \alpha_i(k))].$$

If input signals $\alpha_i(k)$ of the command filter satisfies $|\alpha_i(k+1) - \alpha_i(k)| \leq \varpi_1$ and $|\alpha_i(k+2) - 2\alpha_i(k+1) + \alpha_i(k)| \leq \varpi_2$, where ϖ_1 and ϖ_2 are constants. $|c_{i,1}(k) - \alpha_i(k)| \leq \varrho$, $\Delta c_{i,1}(k) = |c_{i,1}(k+1) - c_{i,1}(k)|$ is bounded for $\varrho > 0$, $0 < \zeta \leq 1$ and $\omega_n > 0$.

Lemma 2 [35]: There are fuzzy logic systems (FLSs) $f(k) = W^T S(Z(k)) + \tau$. $f(k)$ is defined in the compact set. τ is defined as the error, for sufficiently small constants $\varepsilon > 0$, $|\tau| \leq \varepsilon$. $W \in R^N$ is the weight vector. $S(Z(k))$ is the basis function vector, and $S(Z(k))$ satisfied $\lambda_{max}[S(Z(k))^T S(Z(k))] < l$, l is a positive constant.

A. INPUT SATURATION MODEL FOR PMSMs DRIVE SYSTEMS

In the actual operation of the PMSMs, considering the input constraint of the system can improve the system performance and control accuracy. The nonlinear description of input saturation is as following:

$v(k)$ is the saturated nonlinear input signal. $u(k)$ represents the plant input affected by the input saturation nonlinearity.

$$u(k) = \text{sat}(v(k)) = \begin{cases} u_{max}, & v(k) \geq u_{max}, \\ v(k), & u_{min} < v(k) < u_{max}, \\ u_{min}, & v(k) \leq u_{min}, \end{cases}$$

where u_{max} and u_{min} are constants.

Approximate saturation function by using piecewise function.

$$g(v(k)) = \begin{cases} u_{max} \tanh \dfrac{v(k)}{u_{max}}, & v(k) \geq 0, \\ u_{min} \tanh \dfrac{v(k)}{u_{min}}, & v(k) < 0, \end{cases}$$
$$= \begin{cases} u_{max} \dfrac{e^{\frac{v(k)}{u_{max}}} - e^{-\frac{v(k)}{u_{max}}}}{e^{\frac{v(k)}{u_{max}}} + e^{-\frac{v(k)}{u_{max}}}}, & v(k) \geq 0, \\ u_{min} \dfrac{e^{\frac{v(k)}{u_{min}}} - e^{-\frac{v(k)}{u_{min}}}}{e^{\frac{v(k)}{u_{min}}} + e^{-\frac{v(k)}{u_{min}}}}, & v(k) < 0. \end{cases}$$

$\text{sat}(v(k))$ is expressed as $\text{sat}(v(k)) = g(v(k)) + Y(v(k))$, it was defined that $|Y(v(k))| = |\text{sat}(v(k)) - g(v(k))| \leq \max\{u_{max}(1-\tan(1)), u_{min}(\tan(1) - 1)\} = D$, D is a constant and $D > 0$.

In addition, according to the mean-value theorem, there is constant $\lambda(0 < \lambda < 1)$, then

$$g(v(k)) = g(v(0)) + g_{v_\lambda(k)}(v(k) - v(0)),$$

where

$$g_{v_\lambda(k)} = (g(v(k+1)) - g(v(k)))|_{v(k) = v_\lambda(k)},$$

and $v_\lambda(k) = \lambda v(k) + (1 - \lambda)v(0)$.

By defining $v(0) = 0$ and $g(v(0)) = 0$, $g(v(k))$ is again represented as $g(v(k)) = g_{v_\lambda(k)}v(k)$, $0 < g_{v_\lambda(k)} \leq 1$. $u(k)$ is expressed as:

$$u(k) = g_{v_\lambda(k)}v(k) + Y(v(k)). \tag{3}$$

According to Eq.(3), $u_{qs}(k)$ and $u_{ds}(k)$ are described as:

$$\begin{cases} u_{qs}(k) = g_{v_\lambda(k)}v_q(k) + Y(v_q(k)), \\ u_{ds}(k) = g_{v_\lambda(k)}v_d(k) + Y(v_d(k)), \end{cases} \tag{4}$$

where $g_{v_\lambda(k)}$ satisfied $0 < g_{v_\lambda(k)} \leq 1$. $v_q(k)$ and $v_d(k)$ are the input signals of saturation nonlinearity in q-axis and d-axis respectively.

B. REDUCED-ORDER OBSERVER DESIGN

In the traditional control method, rotor angular velocity of PMSMs is measured by the physical sensor. However, the application of physical sensor has some disadvantages such as high cost, noise immunity, low feasibility. In view of the above shortcomings, the rotor angular velocity is estimated by using a reduced-order observer, which replaces the physical sensor.

In system (2), the equation of the subsystem can be obtained as:

$$\begin{cases} \psi_1(k+1) = \psi_1(k) + \Delta_T \psi_2(k), \\ \psi_2(k+1) = \psi_3(k) + f_2(k), \\ y(k) = \psi_1(k), \end{cases} \tag{5}$$

where the unknown nonlinear function $f_2(k) = (1 + \Delta_T a_2(k))\psi_2(k) + a_1\Delta_T\psi_3(k) + a_3\Delta_T\psi_3(k)\psi_4(k) + a_4\Delta_T T_l - \psi_3(k)$. According to lemma 2 [35], there are FLSs $f_2(k) = W_2^T S_2(Z_2(k)) + \tau_2$, τ_2 is defined as approximation error, which satisfies $\tau_2 \leq \varepsilon_2(\varepsilon_2 > 0)$. So Eq. (5) can be recalculated as:

$$\begin{cases} \psi_1(k+1) = \Delta_T \psi_2(k) + \psi_1(k), \\ \psi_2(k+1) = \psi_3(k) + W_2^T S_2(Z_2(k)) + \tau_2, \\ y(k) = \psi_1(k). \end{cases} \tag{6}$$

The adaptive fuzzy observer is constructed as:

$$\begin{cases} \hat{\psi}_1(k+1) = \Delta_T \hat{\psi}_2(k) + \hat{\psi}_1(k) + g_1[y(k) - \hat{y}(k)], \\ \hat{\psi}_2(k+1) = \psi_3(k) + \hat{\chi}_2\|S_2(Z_2(k))\| \\ \quad + g_2[y(k) - \hat{y}(k)], \\ \hat{y}(k) = \hat{\psi}_1(k), \end{cases} \tag{7}$$

where $\|W_2^T\| = \chi_2$, $\chi_2 > 0$, $\hat{\chi}_2 = \chi_2 - \tilde{\chi}_2$ is the estimation of χ_2. $\tilde{\chi}_2$ is the estimation error of χ_2. $Z_2(k) = [\hat{\psi}_1(k), \hat{\psi}_2(k), \psi_3(k), \psi_4(k), \psi_{1d}(k)]^T$.

In order to express the reduced-order observer clearly, equation (7) is written as follows:

$$\begin{cases} \hat{\psi}(k+1) = B\hat{\psi}(k) + Gy + C\psi_3(k) + \tilde{f}, \\ \hat{y}(k) = D^T \hat{\psi}(k), \end{cases} \tag{8}$$

where $B = \begin{bmatrix} -g_1 + 1, & \Delta_T \\ -g_2, & 0 \end{bmatrix}$, $G = \begin{bmatrix} g_1, g_2 \end{bmatrix}^T$, $\hat{\psi}(k) = \begin{bmatrix} \hat{\psi}_1(k), \hat{\psi}_2(k) \end{bmatrix}^T$, $C = \begin{bmatrix} 0, 1 \end{bmatrix}^T$, $D = \begin{bmatrix} 1, 0 \end{bmatrix}^T$, $\tilde{f} = \begin{bmatrix} 0, \hat{\chi}_2 \|S_2(Z_2(k))\| \end{bmatrix}^T$. B is a strict Hurwitz matrix by selecting the appropriate G. $e(k) = \begin{bmatrix} e_1(k), e_2(k) \end{bmatrix}^T$, $e_h(k) = \psi_h(k) - \hat{\psi}_h(k), (h = 1, 2)$, then define the error of the reduced-order observer as:

$$e(k+1) = Be(k) + \varepsilon + \tilde{f}, \tag{9}$$

where $\varepsilon = \begin{bmatrix} 0, \tau_2 \end{bmatrix}^T$. Select $V_0(k) = e^T(k)Pe(k)$ and substitute Eq. (9) into the first-order difference of $V_0(k)$ as follows:

$$\begin{aligned}
\Delta V_0(k) &= e^T(k+1)Pe(k+1) - e^T(k)Pe(k) \\
&= [Be(k) + \varepsilon + \tilde{f}]^T P[Be(k) + \varepsilon + \tilde{f}] \\
&\quad - e^T(k)Pe(k), \\
&\leq -e^T(k)Ye(k) + 3\|P\|^2 \varepsilon_2^2 \\
&\quad + 3\|P\|^2 \tilde{\chi}_2^2(k)\|S_2(Z_2(k))\|^2, \tag{10}
\end{aligned}$$

where $P^T = P > 0$, $Y = P - 3B^T PB$.

III. REDUCED-ORDER OBSERVER-BASED DISCRETE-TIME CFC WITH INPUT CONSTRAINT

In this section, reduced-order observer-based discrete-time CFC method for PMSMs with input constraint and load disturbance will be designed. The block diagram is shown in Fig. 1.
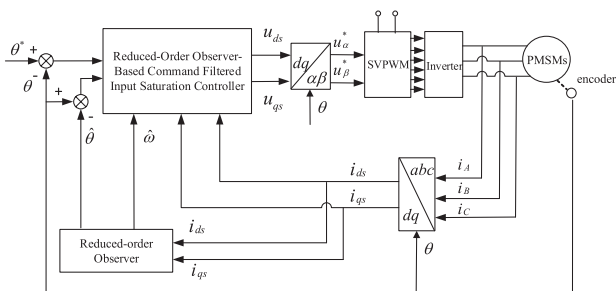

FIGURE 1. Block diagram of reduced-order observer based on input saturation for PMSMs.

Assumption 1: The given reference signal $\psi_{1d}(k)$ and $\psi_{1d}(k+1)$ are known smooth bounded signals.

Define the error signals and the compensating signals as:

$$\begin{cases} e_1(k) = \psi_1(k) - \psi_{1d}(k), \\ e_2(k) = \hat{\psi}_2(k) - c_{1c}(k), \\ e_3(k) = \psi_3(k) - c_{2c}(k), \\ e_4(k) = \psi_4(k), \end{cases} \quad \begin{cases} \xi_1(k) = e_1(k) - \varsigma_1(k), \\ \xi_2(k) = e_2(k) - \varsigma_2(k), \\ \xi_3(k) = e_3(k) - \varsigma_3(k), \\ \xi_4(k) = e_4(k) - \varsigma_4(k), \end{cases}$$

where $c_{1c}(k) = c_{1,1}(k)$ and $c_{2c}(k) = c_{2,1}(k)$ are the output signal, the virtual control function $\alpha_1(k)$ and $\alpha_2(k)$ are defined as the input signals of the command filter. The compensation signal is defined as $\xi_m(k) = e_m(k) - \varsigma_m(k), (m = 1, 2, 3, 4)$. $e_m(k)$ is the tracking error signal. $\varsigma_m(k)$ is compensated error

signals, which is used to compensate the filtering error generated by the first-order filter and improve the control accuracy of the system.

Step 1: Choose the Lyapunov function $V_1(k) = \frac{1}{2}\varsigma_1^2(k)$, $\Delta V_1(k)$ is described as follows:

$$\begin{aligned}
\Delta V_1(k) &= \frac{1}{2}[\psi_1(k) + \Delta_T \hat{\psi}_2(k) \\
&\quad - \psi_{1d}(k+1) - \xi_1(k+1)]^2 - \frac{1}{2}\varsigma_1^2(k). \tag{11}
\end{aligned}$$

Virtual control function $\alpha_1(k)$ is constructed and the compensating signal is adopted as:

$$\alpha_1(k) = \frac{1}{\Delta_T}[\psi_{1d}(k+1) - \psi_1(k)] + t_1\xi_1(k), \tag{12}$$

$$\xi_1(k+1) = \Delta_T[\xi_2(k) + c_{1c}(k) - \alpha_1(k) + t_1\xi_1(k)], \tag{13}$$

where $|t_1| \leq 1$.

Put Eq.(12) and Eq.(13) into Eq.(11) to get:

$$\begin{aligned}
\Delta V_1(k) &= \frac{1}{2}[\Delta_T(\hat{\psi}_2(k) - c_{1c}(k)) - \xi_2(k)]^2 - \frac{1}{2}\varsigma_1^2(k), \\
&\leq \Delta_T^2 \varsigma_2^2(k) + \Delta_T^2 e^T(k)e(k) - \frac{1}{2}\varsigma_1^2(k). \tag{14}
\end{aligned}$$

Remark 1: Using the backstepping method, the virtual controller is selected as: $\alpha_1(k) = \frac{1}{\Delta_T}[\psi_{1d}(k+1) - \psi_1(k)]$, which contains the information of future state $\psi_{1d}(k+1)$. Therefore, the "noncausal problem" appears in the traditional backstepping method.

Step 2: Choose the Lyapunov function $V_2(k) = V_1(k) + \frac{1}{2}\varsigma_2^2(k)$, $\Delta V_2(k)$ is described as follows:

$$\begin{aligned}
\Delta V_2(k) &= \frac{1}{2}[\psi_3(k) + \hat{\chi}_2(k)\|S_2(Z_2(k))\| + g_2 e_0(k) \\
&\quad - c_{1c}(k+1) - \xi_2(k+1)]^2 + \Delta V_1(k) - \frac{1}{2}\varsigma_2^2(k). \tag{15}
\end{aligned}$$

Virtual control function $\alpha_2(k)$ is constructed and the compensating signal is adopted as:

$$\begin{aligned}
\alpha_2(k) &= c_{1c}(k+1) - \hat{\chi}_2(k)\|S_2(Z_2(k))\| \\
&\quad - g_2 e_0(k) + t_2\xi_2(k), \tag{16}
\end{aligned}$$

$$\xi_2(k+1) = \xi_3(k) + c_{2c}(k) - \alpha_2(k) + t_2\xi_2(k), \tag{17}$$

where $|t_2| \leq 1$.

Put Eq.(16) and Eq.(17) into Eq.(15) to get:

$$\begin{aligned}
\Delta V_2(k) &= \frac{1}{2}[\psi_3(k) - \xi_3(k) - c_{2c}(k)]^2 + \Delta V_1(k) \\
&\quad - \frac{1}{2}\varsigma_2^2(k) \\
&= \frac{1}{2}\varsigma_3^2(k) + \Delta V_1(k) - \frac{1}{2}\varsigma_2^2(k). \tag{18}
\end{aligned}$$

Remark 2: By using reduced-order observer, this paper does not need to measure the rotor angular velocity directly. Moreover, system complexity is increased by the use of physical sensor. Reduced-order observer simplifies the complexity of the system and is widely used in practical engineering.

Remark 3: In the traditional backstepping method, $\alpha_1(k)$ includes $\psi_1(k)$ and $\psi_{1d}(k+1)$, and the virtual control function $\alpha_1(k) = \dfrac{\psi_{1d}(k+1) - \psi_1(k)}{\Delta_T}$; Then, $\alpha_2(k)$ contains $\psi_1(k)$, $\psi_2(k)$ and $\alpha_1(k+1)$, and the virtual control function $\alpha_2(k) = \dfrac{-(1 + a_2\Delta_T)\psi_2(k) + \alpha_1(k+1)}{a_1\Delta_T}$. Since $\alpha_1(k+1) = \dfrac{\psi_{1d}(k+2) - \psi_1(k+1)}{\Delta_T}$, $\alpha_2(k) = \dfrac{-(\Delta_T + a_2\Delta_T^2)\psi_2(k) + \psi_{1d}(k+2) - \psi_1(k+1)}{a_1\Delta_T^2}$ is obtained.

Therefore, when the difference of the virtual control function is calculated repeatedly, the "complexity of computation" problem appears. With the increase of system order, the derivation process is also complex. In this paper, the CFC method is developed to effectively solve this problem.

Step 3: Choose the Lyapunov function $V_3(k) = V_2(k) + \frac{1}{2}\varsigma_3^2(k)$, $\Delta V_3(k)$ is expressed as:

$$\Delta V_3(k) = \frac{1}{2}[b_4\Delta_T u_{qs}(k) + f_3(k)]^2 + \Delta V_2(k) - \frac{1}{2}\varsigma_3^2(k), \quad (19)$$

where $f_3(k) = (1 + b_1\Delta_T)\psi_3(k) + b_2\Delta_T\psi_2(k) + b_3\Delta_T\psi_2(k)\psi_4(k) - c_{2c}(k+1) - \xi_3(k+1)$.

According to lemma 2 [35], there are FLSs:

$$f_3(k) = W_3^T S_3(Z_3(k)) + \tau_3, \quad (20)$$

where $Z_3(k) = [\hat{\psi}_1(k), \hat{\psi}_2(k), \psi_3(k), \psi_4(k), \psi_{1d}(k)]^T$, τ_3 is defined as the approximation error and $|\tau_3| \leq \varepsilon_3 (\varepsilon_3 > 0)$.

Remark 4: There are fuzzy logic systems $f_3(k) = W_3^T S_3(Z_3(k)) + \tau_3$. $f_3(k)$ is an unknown nonlinear function. $f_3(k)$ contains the future information $c_{2c}(k+1)$, $\xi_3(k+1)$ and higher order nonlinear functions $\psi_4(k)$ which increase the complexity of the algorithm. Therefore, using FLSs to design controller becomes simple.

With $\xi_3(k) = 0$, the saturated nonlinear input signal $v_q(k)$, the input signal $u_{qs}(k)$ of PMSMs drive systems are selected as:

$$\begin{cases} v_q(k) = -\dfrac{1}{b_4\Delta_T}\hat{W}_3(k) \|S_3(Z_3(k))\|, \\ u_{qs}(k) = g_{v_\lambda(k)}v_q(k) + Y(v_q(k)), \end{cases} \quad (21)$$

where $g_{v_\lambda(k)} = 1$. Define $\|W_3^T\| = \chi_3 (\chi_3 > 0)$. $\tilde{\chi}_3(k) = \chi_3 - \hat{\chi}_3(k)$ is an estimation error.

The adaptive law $\hat{\chi}_3(k+1)$ are chosen as:

$$\hat{\chi}_3(k+1) = \hat{\chi}_3(k) + \iota_3 \|S_3(Z_3(k))\|\varsigma_3(k+1) - \eta_3\hat{\chi}_3(k), \quad (22)$$

where ι_3 and η_3 are positive parameters which greater than 0. Substitute Eq.(20) and Eq.(21) into Eq.(19) to obtain:

$$\Delta V_3(k) = \frac{1}{2}[\tilde{W}_3(k) \|S_3(Z_3(k))\| + \tau_3 + b_4\Delta_T D]^2 + \Delta V_2(k) - \frac{1}{2}\varsigma_3^2(k),$$

$$\leq 2\tilde{\chi}_3^2(k)\|S_3(Z_3(k))\|^2 + 2b_4^2\Delta_T^2 D^2 + \varepsilon_3^2 + \Delta V_2(k) - \frac{1}{2}\varsigma_3^2(k). \quad (23)$$

Step 4: Choose the Lyapunov function $V_4(k) = V_3(k) + \frac{M}{2}\varsigma_4^2(k)$, where $M > 0$, $\Delta V_4(k)$ is described as follows:

$$\Delta V_4(k) = \frac{M}{2}[c_3\Delta_T u_{ds}(k) + f_4(k)]^2 + \Delta V_3(k) - \frac{M}{2}\varsigma_4^2(k), \quad (24)$$

where $f_4(k) = (1 + c_1\Delta_T)\psi_4(k) + c_2\Delta_T\psi_2(k)\psi_3(k) - \xi_4(k+1)$.

According to lemma 2 [35], there are FLSs:

$$f_4(k) = W_4^T S_4(Z_4(k)) + \tau_4, \quad (25)$$

where $Z_4(k) = [\hat{\psi}_1(k), \hat{\psi}_2(k), \psi_3(k), \psi_4(k), \psi_{1d}(k)]^T$, τ_4 is defined as the approximation error and $|\tau_4| \leq \varepsilon_4 (\varepsilon_4 > 0)$.

With $\xi_4(k) = 0$, the saturated nonlinear input signal $v_d(k)$, the input signal $u_{ds}(k)$ of PMSMs drive systems are selected as:

$$\begin{cases} v_d(k) = -\dfrac{1}{c_3\Delta_T}\hat{\chi}_4(k) \|S_4(Z_4(k))\|, \\ u_{ds}(k) = g_{v_\lambda(k)}v_d(k) + Y(v_d(k)), \end{cases} \quad (26)$$

where $g_{v_\lambda(k)} = 1$. Define $\|W_4^T\| = \chi_4 (\chi_4 > 0)$. $\tilde{\chi}_4(k) = \chi_4 - \hat{\chi}_4(k)$ is an estimation error.

The adaptive law $\hat{\chi}_4(k+1)$ are chosen as:

$$\hat{\chi}_4(k+1) = \hat{\chi}_4(k) + \iota_4 \|S_4(Z_4(k))\|\varsigma_4(k+1) - \eta_4\hat{\chi}_4(k), \quad (27)$$

where ι_4 and η_4 are positive parameters.

Substitute Eq.(25) and Eq.(26) into Eq.(24) to obtain:

$$\Delta V_4(k) = \frac{M}{2}\left[\tilde{\chi}_4(k) \|S_4(Z_4(k))\| + \tau_4 + c_3\Delta_T D\right]^2 + \Delta V_3(k) - \frac{M}{2}\varsigma_4^2(k),$$

$$\leq -\frac{M}{2}\varsigma_4^2(k) - \frac{1}{2}\left(1 - \Delta_T^2\right)\varsigma_2^2(k) - \frac{1}{2}\varsigma_1^2(k) + \varepsilon_3^2 + 2M\tilde{\chi}_4^2(k)\|S_4(Z_4(k))\|^2 + 2\tilde{\chi}_3^2(k)\|S_3(Z_3(k))\|^2 + 2M + c_3^2\Delta_T^2 D^2 + M\varepsilon_4^2 + 2b_4^2\Delta_T^2 D^2. \quad (28)$$

Next, it is proved that the closed-loop system is semi-globally uniformly ultimately bounded by Lyapunov stability analysis. Theorem 1 is shown as follows:

Theorem 1: For discrete-time systems (2) under Assumptions 1 and the given signal ψ_{1d}, the reduced-order observer (8), the nonlinear input saturation controllers (21) and (26), the virtual control functions (12) and (16), compensating signals (13) and (17), the adaptive laws (22) and (27) can guarantee that the position tracking error can converge a small neighborhood of the origin and all closed-loop signals are semi-globally uniformly ultimately bounded. The proof of detail is given as follows:

Proof: In order to verify the feasibility of the command filtered discrete-time control method proposed in this paper, Lyapunov function is used as follows:

$$V(k) = V_0(k) + V_4(k) + \frac{1}{2\iota_2}\tilde{\chi}_2^2(k) + \frac{1}{2\iota_3}\tilde{\chi}_3^2(k) + \frac{M}{2\iota_4}\tilde{\chi}_4^2(k).$$

The first-order difference of $V(k)$ is expressed as:

$$\Delta V(k)$$
$$= \Delta V_0(k) + \Delta V_4(k) + \frac{1}{2\iota_2}[\tilde{\chi}_2^2(k+1) - \tilde{\chi}_2^2(k)]$$
$$+ \frac{1}{2\iota_3}[\tilde{\chi}_3^2(k+1) - \tilde{\chi}_3^2(k)] + \frac{M}{2\iota_4}[\tilde{\chi}_4^2(k+1) - \tilde{\chi}_4^2(k)].$$
$$(29)$$

According to $\tilde{\chi}_n(k+1) = \chi_n - \hat{\chi}_n(k+1)(n = 2, 3, 4)$, the adaptive laws (22) and (27), the following can be obtained:

$$\tilde{\chi}_n^2(k+1) - \tilde{\chi}_n^2(k)$$
$$= \chi_n^2 + (1 - \eta_n)^2\hat{\chi}_n^2(k)$$
$$+ \iota_n^2\|S_n(Z_n(k))\|^2\varsigma_n^2(k+1)$$
$$+ 2(1 - \eta_n)\iota_n\|S_n(Z_n(k))\|\varsigma_n(k+1)\hat{\chi}_n(k)$$
$$- \tilde{\chi}_n^2(k) - 2\iota_n\|S_n(Z_n(k))\|\varsigma_n(k+1)\chi_n$$
$$- 2(1 - \eta_n)\chi_n\hat{\chi}_n(k).$$
$$(30)$$

Using $\|S_n(Z_n(k))\| \leq l_n$ and according to Young's inequality:

$$2\iota_n\|S_n(Z_n(k))\|\varsigma_n(k+1)\hat{\chi}_n(k) \leq \varsigma_n^2(k+1)l_n$$
$$+ \iota_n\hat{\chi}_n^2(k),$$
$$-2\|S_n(Z_n(k))\|\varsigma_n(k+1)\chi_n \leq \varsigma_n^2(k+1)l_n + \chi_n^2,$$
$$\iota_n^2\|S_n(Z_n(k))\|^2\varsigma_n^2(k+1) \leq \iota_n^2\varsigma_n^2(k+1)l_n,$$
$$-2\chi_n\hat{\chi}_n(k) \leq \hat{\chi}_n^2(k) + \chi_n^2. \quad (31)$$

According to $\varsigma_p(k) = e_p(k) - \xi_p(k)(p = 3, 4)$, Eq.(1), Eq.(20), Eq.(25) and Young's inequality, the compensation error signal is described as:

$$\begin{cases} \varsigma_3^2(k+1) \leq 4\tilde{\chi}_3^2 l_3 + 4b_4^2\Delta_T^2 D^2 + 2\varepsilon_3^2, \\ \varsigma_4^2(k+1) \leq 4\tilde{\chi}_4^2 l_4 + 4c_3^2\Delta_T^2 D^2 + 2\varepsilon_4^2. \end{cases} \quad (32)$$

Put Eq.(31) and Eq.(32) into Eq.(30) to get:

$$\tilde{\chi}_2^2(k+1) - \tilde{\chi}_2^2(k)$$
$$\leq \hat{\chi}_2^2(k)\left(2 + \eta_2^2 - \eta_2(3 + \iota_2) + \iota_2\right)$$
$$+ \chi_2^2(\iota_2 - \eta_2 + 2) - \tilde{\chi}_2^2(k) + \varsigma_3(k)(l_2(1 - \eta_2 + \iota_2)).$$
$$(33)$$

$$\tilde{\chi}_3^2(k+1) - \tilde{\chi}_3^2(k)$$
$$\leq \hat{\chi}_3^2(k)\left(2 + \eta_3^2 - \eta_3(3 + \iota_3) + \iota_3\right)$$
$$+ \chi_3^2(\iota_3 - \eta_3 + 2) + 4b_4^2\Delta_T^2 D^2(l_3 - l_3\eta_3 + l_3\iota_3)$$
$$+ \tilde{\chi}_3^2(k)\left(4l_3^2 - 4l_3^2\eta_3 + 4l_3^2\iota_3 - 1\right)$$
$$+ 2\varepsilon_3^2(l_3 - l_3\eta_3 + l_3\iota_3). \quad (34)$$

$$\tilde{\chi}_4^2(k+1) - \tilde{\chi}_4^2(k)$$
$$\leq \hat{\chi}_4^2(k)\left(2 + \eta_4^2 - \eta_4(3 + \iota_4) + \iota_4\right)$$
$$+ \chi_4^2(\iota_4 - \eta_4 + 2) + 4c_3^2\Delta_T^2 D^2(l_4 - l_4\eta_4 + l_4\iota_4)$$
$$+ \tilde{\chi}_4^2(k)\left(4l_4^2 - 4l_4^2\eta_4 + 4l_4^2\iota_4 - 1\right)$$
$$+ 2\varepsilon_4^2(l_4 - l_4\eta_4 + l_4\iota_4). \quad (35)$$

Put Eq.(28), Eq.(33), Eq.(34)and Eq.(35) into Eq.(29) to get:

$$\Delta V \leq -e^T(k)(Y - \Delta_T^2)e(k) - \frac{M}{2}\varsigma_4^2(k) - \frac{1}{2}\varsigma_1^2(k)$$
$$- \frac{1}{2\iota_2}(l_2\eta_2 - l_2 - l_2\iota_2)\varsigma_3^2(k) - \frac{1}{2}\left(1 - 2\Delta_T^2\right)\varsigma_2^2(k)$$
$$+ \frac{1}{2\iota_2}[(2 + \eta_2^2 - \eta_2(3 + \iota_2) + \iota_2)\hat{\chi}_2^2(k)$$
$$+ (6\iota_2\|P\|^2 - 1)\tilde{\chi}_2^2 + \beta_2]$$
$$+ \frac{1}{2\iota_3}[(2 + \eta_3^2 - \eta_3(3 + \iota_3) + \iota_3)\hat{\chi}_3^2(k) + \beta_3$$
$$+ (4l_3^2 - 4l_3^2\eta_3 + 4l_3^2\iota_3 + 4l_3\iota_3 - 1)\tilde{\chi}_3^2(k)]$$
$$+ \frac{M}{2\iota_4}[(2 + \eta_4^2 - \eta_4(3 + \iota_4) + \iota_4)\hat{\chi}_4^2(k) + \beta_4$$
$$+ (4l_4^2 - 4l_4^2\eta_4 + 4l_4^2\iota_4 + 4l_4\iota_4 - 1)\tilde{\chi}_4^2(k)]. \quad (36)$$

where

$$\begin{cases} \beta_2 = (\iota_2 - \eta_2 + 2)\chi_2^2 + 6\iota_2\|P\|^2\varepsilon_2^2, \\ \beta_3 = (\iota_3 - \eta_3 + 2)\chi_3^2 + 2\varepsilon_3^2(l_3 - l_3\eta_3 + l_3\iota_3) \\ \quad + 4b_4^2\Delta_T^2 D^2(l_3 - l_3\eta_3 + l_3\iota_3 + \iota_3/2), \\ \beta_4 = (\iota_4 - \eta_4 + 2)\chi_4^2 + 2\varepsilon_4^2(l_4 - l_4\eta_4 + l_4\iota_4) \\ \quad + 4c_3^2\Delta_T^2 D^2(l_4 - l_4\eta_4 + l_4\iota_4 + M\iota_4/2). \end{cases}$$

By choosing the appropriate parameters M, ι_3, ι_4, η_3 and η_4, the inequality are satisfied: $1 - 2\Delta_T^2 > 0$, $l_2\eta_2 - l_2 - l_2\iota_2 > 0$, $4l_h^2 - 4l_h^2\eta_h + 4l_h^2\iota_h + 4l_h\iota_h - 1 < 0(h = 3, 4)$, $2 + \eta_j^2 - \eta_j(3 + \iota_j) + \iota_j < 0(j = 2, 3, 4)$ and Y is positive definite. If the error $|\varsigma_2(k)| > \sqrt{\frac{\beta_2}{2\iota_2(1-2\Delta_T^2)}}$, $|\varsigma_3(k)| > \sqrt{\frac{\beta_3\iota_2}{\iota_3 l_2(\eta_2-1-\iota_2)}}$ and $|\varsigma_4(k)| > \sqrt{\frac{\beta_4}{M\iota_4}}$, then $\Delta V(k) \leq 0$, which means $\lim_{k\to\infty}\|\varsigma_1(k)\| \leq \sigma$ for a small constant $\sigma > 0$. Assuming $c_{ic}(k) - \alpha_i(k)$ are bounded and $|t_i| < 1$. Thus the compensation signal $\xi_i(k)(i = 1, 2)$ is bounded. Since $\varsigma_1(k) = e_1(k) - \xi_1(k)$ and $\xi_1(k)$ are bounded. Then it can get that $e_1(k)$ is bounded. From Eq.(36), the conclusion is summarized as follows:

$$\Delta V(k) \leq -aV(k) + b \quad (37)$$

where

$$a = \min\{l_2\eta_2 - l_2 - l_2\iota_2, 1 - 2\Delta_T^2, Y - \Delta_T^2\},$$
$$b = \frac{1}{2\iota_2}[(2 + \eta_2^2 - \eta_2(3 + \iota_2) + \iota_2)\hat{\chi}_2^2(k) + (6\iota_2\|P\|^2 - 1)\tilde{\chi}_2^2 + \beta_2]$$
$$+ \frac{1}{2\iota_3}[(2 + \eta_3^2 - \eta_3(3 + \iota_3) + \iota_3)\hat{\chi}_3^2(k) + \beta_3$$
$$+ (4l_3^2 - 4l_3^2\eta_3 + 4l_3^2\iota_3 + 4l_3\iota_3 - 1)\tilde{\chi}_3^2(k)]$$
$$+ \frac{M}{2\iota_4}[(2 + \eta_4^2 - \eta_4(3 + \iota_4) + \iota_4)\hat{\chi}_4^2(k) + \beta_4$$
$$+ (4l_4^2 - 4l_4^2\eta_4 + 4l_4^2\iota_4 + 4l_4\iota_4 - 1)\tilde{\chi}_4^2(k)].$$
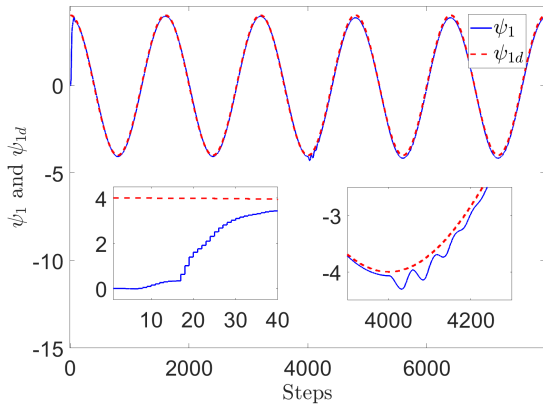
FIGURE 2. Trajectory of the ψ_1 and ψ_{1d} (CFC).

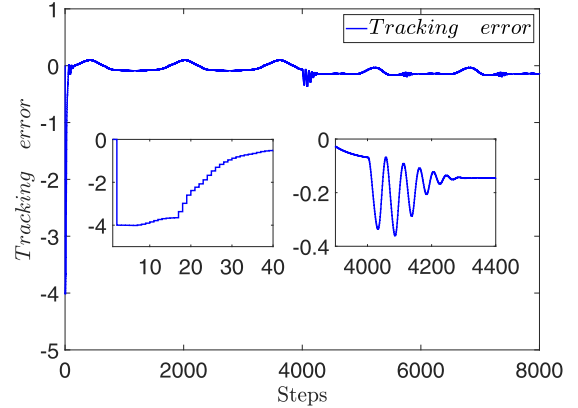**FIGURE 3.** Trajectory of the ψ_1 and ψ_{1d} (DSC).

FIGURE 4. Noise disturbance d(t).

FIGURE 5. Tracking error e_1 (CFC).

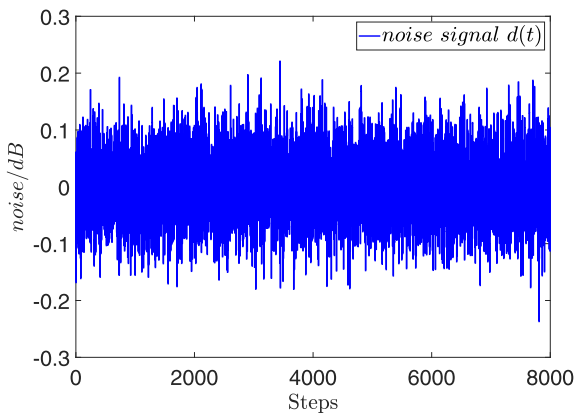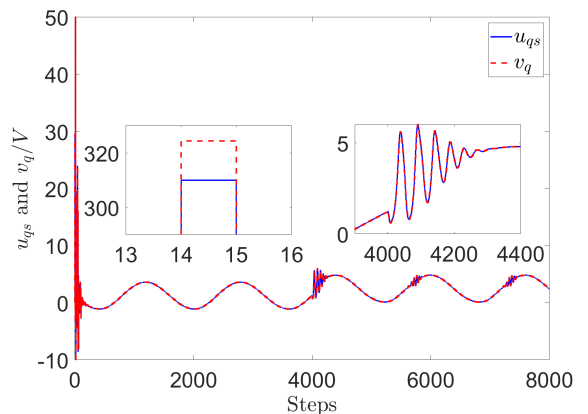**FIGURE 6.** Tracking error e_1 (DSC).

FIGURE 7. The controller u_{qs} (CFC).

According to reference [8], $V(k)$ satisfies:

$$V(k) \leq \frac{\lambda_2}{\lambda_1}\|V(0)\|^2(1-a)^k + \frac{b}{\lambda_1 a}$$

where $V(0)$ is the given initial of $V(k)$, $\lambda_1 > 0$, $\lambda_2 > 0$, $0 < a < 1$, $b \geq 0$.

Finally, all closed-loop signals are proved to be semi-globally uniformly ultimately bounded.

Remark 5: It can be seen from the definition of a and b that parameters $\eta_2, \eta_3, \eta_4, \iota_2, \iota_3, \iota_4$ are selected to ensure $0 < a < 1$ and $b \geq 0$. In order to meet $\left\{|\varsigma_2(k)| > \sqrt{\frac{\beta_2}{2\iota_2(1-2\Delta_T^2)}}, |\varsigma_3(k)| > \sqrt{\frac{\beta_3 \iota_2}{\iota_3 l_2(\eta_2 - 1 - \iota_2)}}, |\varsigma_4(k)| > \sqrt{\frac{\beta_4}{M\iota_4}}\right\}$, large control parameters $\iota_2, \iota_3, \iota_4$ and small control parameters $\beta_2, \beta_3, \beta_4$ are selected.
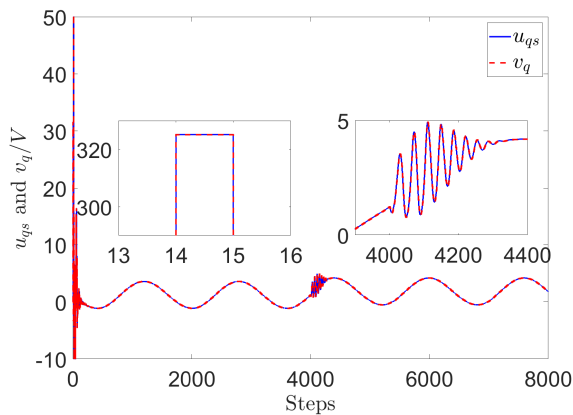
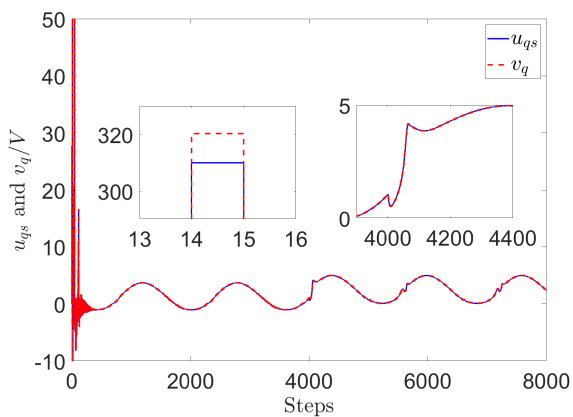**FIGURE 8.** The controller without input constraint u_{qs} (CFC).
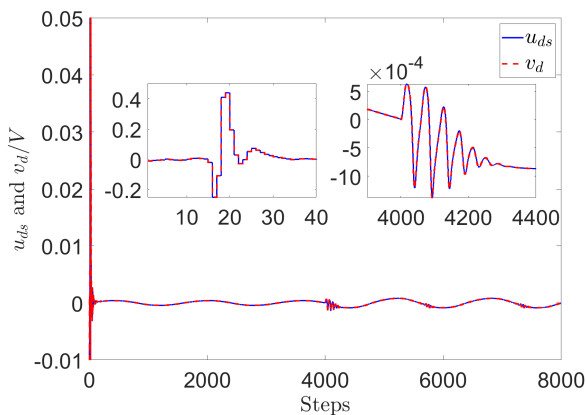

FIGURE 9. The controller u_{qs} (DSC).

FIGURE 10. The controller u_{ds} (CFC).

TABLE 2. Parameters of PMSMs.

Name	Unit	Value
l_d	H	0.00315
l_q	H	0.00258
R_s	Ω	0.68
n_p	/	3
J	$Kg \cdot m^2$	0.003795
B	$N \cdot m/(rad/s)$	0.001158
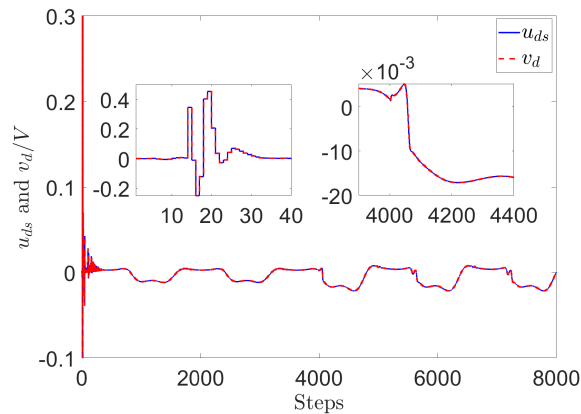
FIGURE 11. The controller u_{ds} (DSC).
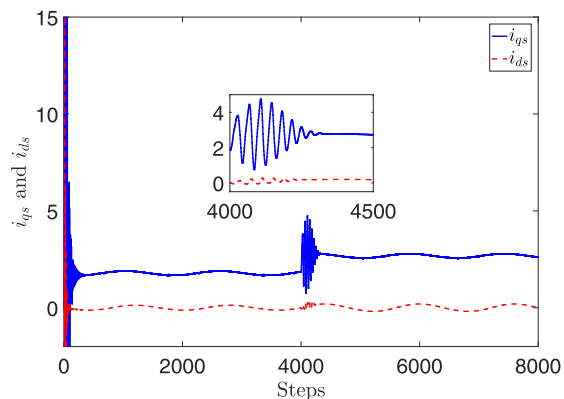
FIGURE 12. Current signals for i_{qs} and i_{ds} (CFC).

IV. SIMULATION AND EXPERIMENT

A. SIMULATION RESULTS

In the simulation part, the CFC method is compared with the DSC method for PMSMs drive systems. The parameters are selected in Table 2.

In this paper, the purpose of designing the controller is that rotor position $\psi_1(k)$ can track given signal $\psi_{1d}(k)$ quickly and effectively. The reference signal is selected as: $\psi_{1d}(k) = 4\cos(\Delta_T k \pi/2)$. Choosing a smaller sampling time is conducive to improving the control accuracy of the system, $\Delta_T = 0.0025$s. The initial value of system (2) is defined as: $\psi_1(0) = \psi_2(0) = \psi_3(0) = \psi_4(0) = 0$. The load torque is described as: when $k < 4000$, T_l is $1.0\,N \cdot m$. When $k \geq 4000$, T_l is $2\,N \cdot m$.

The selection of fuzzy logic systems are as follows: $\mu_{F_i^b} = \exp[\frac{-(\hat{\psi}_i(k)+l)}{2}]$ ($i = 1, 2$) and $\mu_{F_j^b} = \exp[\frac{-(\psi_j(k)+l)}{2}]$($j = 3, 4$) contain eleven nodes $b \in [1, 11]$ with $l \in [-10, 10]$.
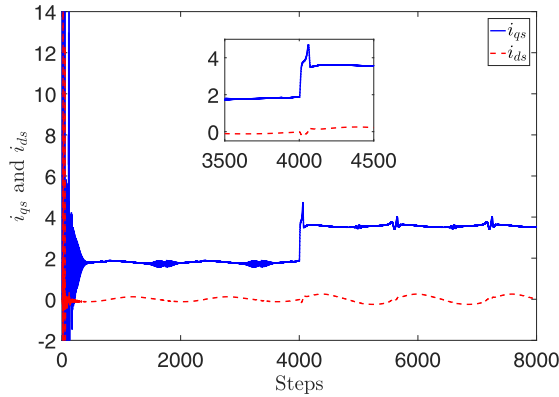
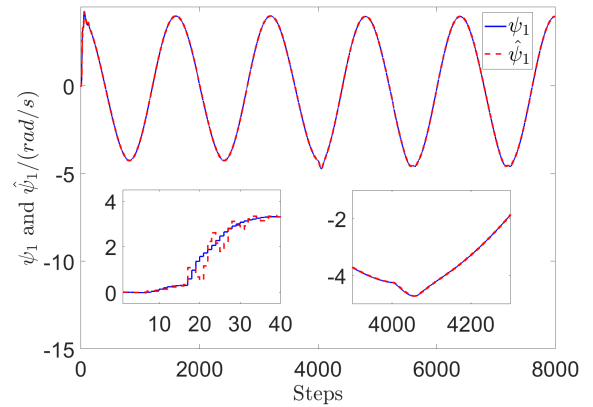**FIGURE 13. Current signals for i_{qs} and i_{ds} (DSC).**
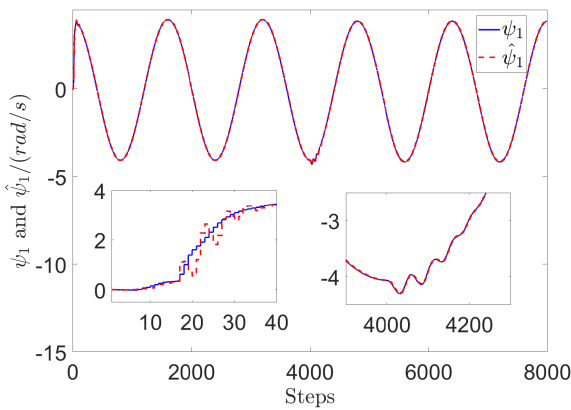

FIGURE 15. $\hat{\psi}_1$ (DSC).

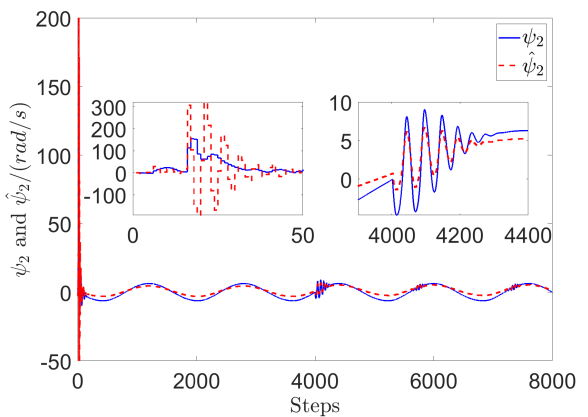**FIGURE 14. $\hat{\psi}_1$ (CFC).**

FIGURE 16. $\hat{\psi}_2$ (CFC).

In order to emphasize the rationality of the CFC method, the CFC method and the DSC method are compared in this paper.

(a) In the simulation, the CFC method is applied to the PMSMs drive systems, and the design parameters are selected as: $\zeta = 0.478, w_n = 295, \iota_2 = 0.1430, \iota_3 = 0.0006, \iota_4 = 0.0001, \eta_2 = 0.5514, \eta_3 = 0.2581, \eta_4 = 0.7991, g_1 = 0.4907, g_2 = 300$.

(b) The DSC method is compared with the CFC method. Both methods select the same optimal control parameters.

The simulation results are shown in Figs. 2∼17. The CFC method with input constraint is illustrated in Figs. 2, 5, 7, 8, 10, 12, 14, 16. By comparison, Figs. 3, 6, 9, 11, 13, 15, 17 reflect the DSC method with input constraint. Trajectory of the $\psi_1(k)$ and $\psi_{1d}(k)$ are given in Fig. 2 and Fig. 3. It can be seen that the tracking effect of Fig. 3 is better than that of Fig. 2. The noise disturbance signal $d(t)$ is shown in Fig. 4. The tracking error curves $e_1(k)$ is given in Fig. 5 and Fig. 6 for the noise disturbance signal. The tracking error fluctuation curve of the CFC method is smaller than that of the DSC method, so the CFC method has better tracking effect and can improve the control accuracy of the system. The curves of q−axis voltage $u_{qs}(k)$ is designed in Fig. 7, Fig. 8 and Fig. 9. It is obvious that the controller

in Fig. 8 does not fully consider the input saturation problem. Fig. 7 and Fig. 9 are comparative figures of the CFC method and the DSC method. Although both methods can limit the voltage to a reasonable range, the DSC method has a large fluctuation near the zero point, which makes the PMSMs run unstable and reduces the control effect of the system. Fig. 10 and Fig. 11 are the curves of d−axis voltage $u_{ds}(k)$. The voltage fluctuation amplitude of the DSC method used in Fig. 11 is relatively large. Fig. 12 and Fig. 13 show the comparison of q-axis and d-axis current figures through CFC and DSC method. The actual and estimated values of the rotor position and rotor angular velocity are shown in Fig. 14 ∼ Fig. 17 for the CFC and the DSC method. As can be seen from Fig. 2 ∼ Fig. 17, the tracking effect of the CFC method is better than that of the DSC method and the control performance is good. The CFC method is more conducive to industrial production.

Remark 6: It can be seen that Fig. 8 does not consider the problem of input saturation, which will seriously affect the control performance of the PMSMs. In Fig. 7, the input saturation problem is considered, which can improve the control effect of the motor and is suitable for practical applications.
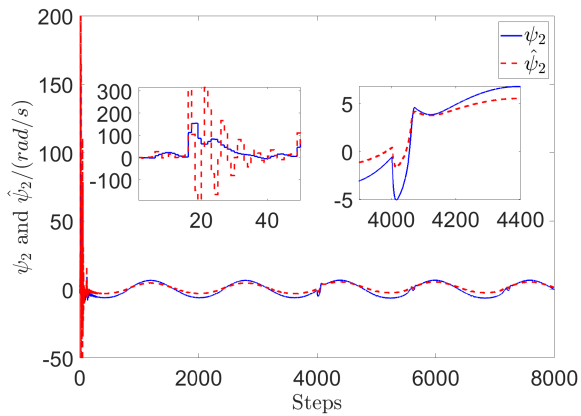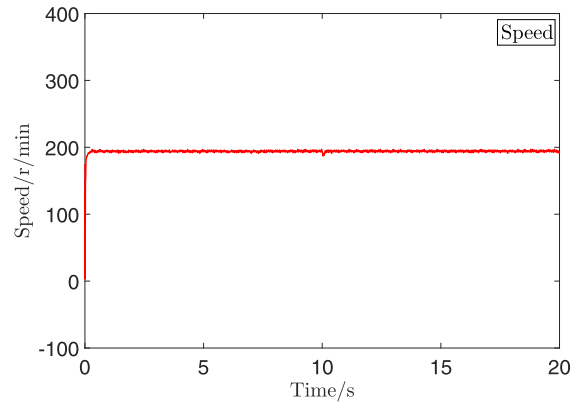
FIGURE 17. $\hat{\psi}_2$ (DSC).
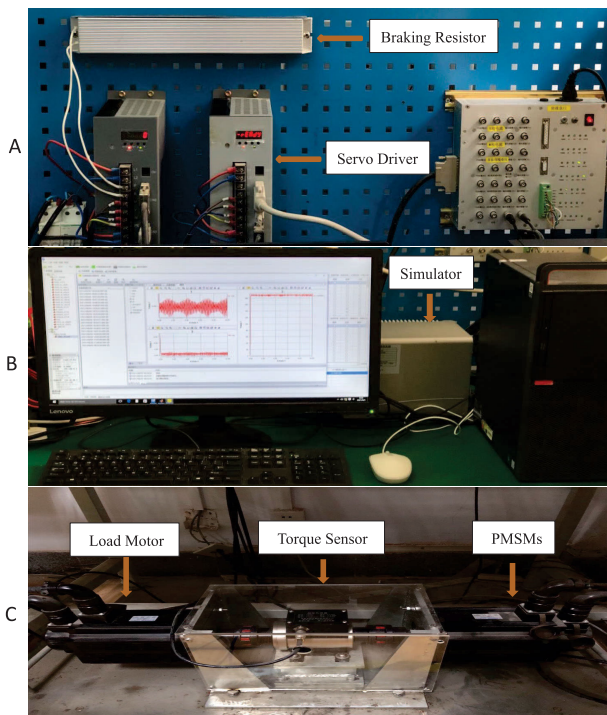

FIGURE 18. Experimental platform.

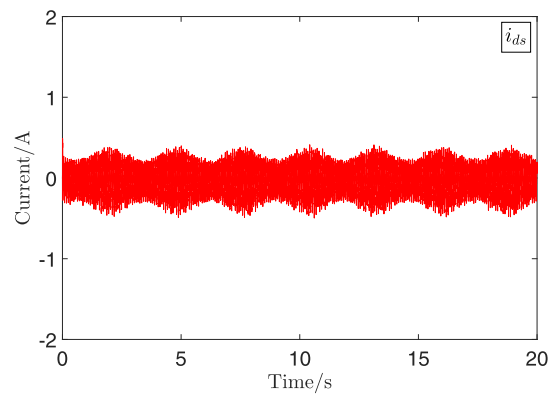**FIGURE 19.** Speed curves.

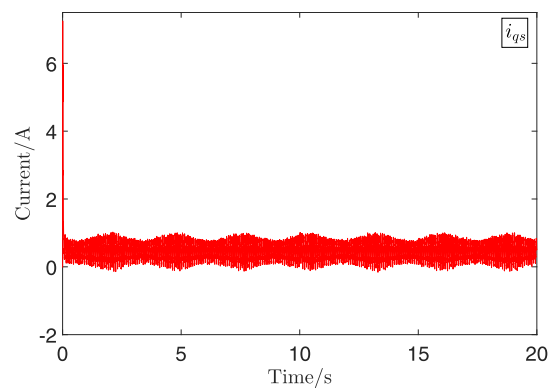

FIGURE 20. Current curve i_{ds}.

FIGURE 21. Current curve i_{qs}.

Remark 7: As can be seen from Fig. 2 to Fig. 3, the control method based on CFC and DSC can track the reference signal ψ_{1d} when the input saturation problem occurs. However, Fig. 2 shows that the tracking error is small because the error compensation mechanism is introduced into this paper. Compared with the DSC method, CFC method used in this paper has better tracking performance and is more suitable for practice industry.

Remark 8: It can be seen from Fig. 5 and Fig. 6 that the control method adopted in this paper can not only overcome the influence of load disturbance and noise disturbance, but also have small tracking error and anti-interference ability.

Remark 9: Note that the proposed discrete-time command filtered control method has good position tracking performance without considering the iron losses. This work is only a preliminary conclusion and will consider how to reduce the above restriction. The traditional sampling control wastes computing resources. The combination of ET mechanism and command filtered control method can not only reduce the update frequency of the system, but also save computing resources, which has important practical significance.

B. EXPERIMENTAL RESULTS

In this part, the experimental results of the PMSMs are presented and analyzed. A non-salient pole PMSMs based on
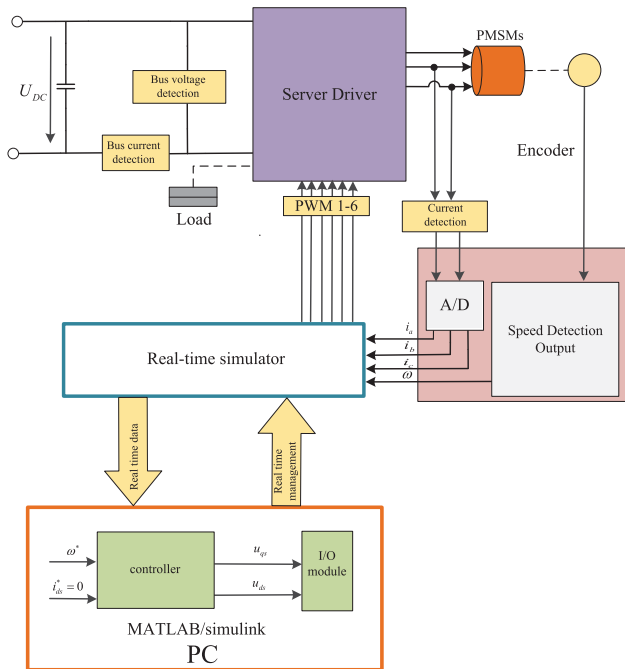
FIGURE 22. A block diagram of the experimental setup.

130MB150A type was used in experiment. The controller is the LINKS-RT rapid prototyping system. The simulator be able to realize the simulation model. The parameters of the motor are: rated speed is 1000r/min, rated torque is 14.5 N · m, rated power is 1.5kW, rated current is 7.3A. The experimental platform consists of hardware and software, as shown in Fig. 18, which is divided into three parts: A, B and C. The block diagram of the experimental setup is shown in Fig. 22. In order to verify the feasibility of the proposed control strategy, the experimental results are shown in Fig. 19, Fig. 20 and Fig. 21. When t < 10s, the load disturbance is 1N · m. When t = 10s, the load disturbance increases rapidly to 2N · m. The given reference speed is 200r/min. Fig. 19 shows the corresponding speed curve. Fig. 20 and Fig. 21 represent d-axis and q-axis current curves respectively. The current fluctuation is small, which makes the motor run more smoothly. The above experimental results show that the proposed control method has small speed fluctuation and strong anti-interference ability.

V. CONCLUSION

For the discrete-time system of PMSMs, this paper has proposed adaptive fuzzy observer based on command filtered control method for input constraint and load disturbance. The rotor angular velocity is estimated by using a reduced-order observer. The unknown nonlinear function is approximated by FLSs. The "complexity of computation" problem is solved by using command filtered control method, and the filtering error is eliminated by using error compensation mechanism. The stability analysis shows that all closed-loop signals are semi-globally uniformly ultimately bounded. The simulation

results confirmed that the designed controller can consider the influence of input constraint and load disturbance, so that the designed controller has strong robustness and ensures good tracking performance. In the future, we will combine the event-triggered mechanism with the CFC method and apply it to practical industry.

REFERENCES

[1] B. Sarsembayev, K. Suleimenov, and T. D. Do, "High order disturbance observer based PI-PI control system with tracking anti-windup technique for improvement of transient performance of PMSM," *IEEE Access*, vol. 9, pp. 66323–66334, 2021.

[2] X. Liu, H. Yu, J. Yu, and L. Zhao, "Combined speed and current terminal sliding mode control with nonlinear disturbance observer for PMSM drive," *IEEE Access*, vol. 6, pp. 29594–29601, 2018.

[3] X. Liu, H. Yu, J. Yu, and Y. Zhao, "A novel speed control method based on port-controlled Hamiltonian and disturbance observer for PMSM drives," *IEEE Access*, vol. 7, pp. 111115–111123, 2019.

[4] H. Li, L. Wang, H. Du, and A. Boulkroune, "Adaptive fuzzy backstepping tracking control for strict-feedback systems with input delay," *IEEE Trans. Fuzzy Syst.*, vol. 25, no. 3, pp. 642–652, Jun. 2017.

[5] H. Wang, B. Chen, X. Liu, K. Liu, and C. Lin, "Robust adaptive fuzzy tracking control for pure-feedback stochastic nonlinear systems with input constraints," *IEEE Trans. Cybern.*, vol. 43, no. 6, pp. 2093–2104, Dec. 2013.

[6] J. Yu, P. Shi, W. Dong, B. Chen, and C. Lin, "Neural network-based adaptive dynamic surface control for permanent magnet synchronous motors," *IEEE Trans. Neural Netw. Learn. Syst.*, vol. 26, no. 3, pp. 640–645, Mar. 2014.

[7] T. Zhang, S. S. Ge, and C. C. Hang, "Adaptive neural network control for strict-feedback nonlinear systems using backstepping design," *Automatica*, vol. 36, no. 12, pp. 1835–1846, 2000.

[8] F. Yang, Z. Wang, Y. Hung, and M. Gani, "H ∞ control for networked systems with random communicatio," *IEEE Trans. Autom. Control*, vol. 51, no. 3, pp. 511–518, Mar. 2006.

[9] H. Li, J. Wang, and P. Shi, "Output-feedback based sliding mode control for fuzzy systems with actuator saturation," *IEEE Trans. Fuzzy Syst.*, vol. 24, no. 6, pp. 1282–1293, Dec. 2016.

[10] O. Mofid, S. Mobayen, and W. K. Wong, "Adaptive terminal sliding mode control for attitude and position tracking control of quadrotor UAVs in the existence of external disturbance," *IEEE Access*, vol. 9, pp. 3428–3440, 2021.

[11] X. Su, X. Liu, P. Shi, and R. Yang, "Sliding mode control of discrete-time switched systems with repeated scalar nonlinearities," *IEEE Trans. Autom. Control*, vol. 62, no. 9, pp. 4604–4610, Sep. 2017.

[12] X. Zhao, H. Yang, W. Xia, and X. Wang, "Adaptive fuzzy hierarchical sliding-mode control for a class of MIMO nonlinear time-delay systems with input saturation," *IEEE Trans. Fuzzy Syst.*, vol. 25, no. 5, pp. 1062–1077, Oct. 2017.

[13] B. Qiu, G. Wang, Y. Fan, D. Mu, and X. Sun, "Adaptive course control-based trajectory linearization control for uncertain unmanned surface vehicle under rudder saturation," *IEEE Access*, vol. 7, pp. 108768–108780, 2019.

[14] S. Khorashadizadeh and M. Sadeghijaleh, "Adaptive fuzzy tracking control of robot manipulators actuated by permanent magnet synchronous motors," *Comput. Electr. Eng.*, vol. 72, pp. 100–111, Nov. 2018.

[15] S. Shao, M. Chen, and Y. Zhang, "Adaptive discrete-time flight control using disturbance observer and neural networks," *IEEE Trans. Neural Netw. Learn. Syst.*, vol. 30, no. 12, pp. 3708–3721, Dec. 2019.

[16] W. Sun, Z. Zhao, and H. Gao, "Saturated adaptive robust control for active suspension systems," *IEEE Trans. Ind. Electron.*, vol. 60, no. 9, pp. 3889–3896, Sep. 2013.

[17] H. Wang, S. Kang, and Z. Feng, "Finite-time adaptive fuzzy command filtered backstepping control for a class of nonlinear systems," *Int. J. Fuzzy Syst.*, vol. 21, no. 8, pp. 2575–2587, Nov. 2019.

[18] Y. Han, J. Yu, L. Zhao, H. Yu, and C. Lin, "Finite-time adaptive fuzzy control for induction motors with input saturation based on command filtering," *IET Control Theory Appl.*, vol. 12, no. 15, pp. 2148–2155, 2018.

[19] J. Wang, C. Wang, Y. Wei, and C. Zhang, "Command filter based adaptive neural trajectory tracking control of an underactuated underwater vehicle in three-dimensional space," *Ocean Eng.*, vol. 180, pp. 175–186, May 2019.

[20] G. Cui, J. Yu, and Q.-G. Wang, "Finite-time adaptive fuzzy control for MIMO nonlinear systems with input saturation via improved command-filtered backstepping," *IEEE Trans. Syst., Man, Cybern. Syst.*, early access, Aug. 6, 2021, doi: 10.1109/TSMC.2020.3010642.

[21] W. Xie, G. Yu, D. Cabecinhas, R. Cunha, and C. Silvestre, "Global saturated tracking control of a quadcopter with experimental validation," *IEEE Control Syst. Lett.*, vol. 5, no. 1, pp. 169–174, Jan. 2021.

[22] K. Shojaei, "Output-feedback formation control of wheeled mobile robots with actuators saturation compensation," *Nonlinear Dyn.*, vol. 89, no. 4, pp. 2867–2878, Sep. 2017.

[23] O. Garcia-Alarcon and J. Moreno-Valenzuela, "Analysis and design of a controller for an input-saturated DC–DC buck power converter," *IEEE Access*, vol. 7, pp. 54261–54272, 2019.

[24] W. Gao and R. R. Selmic, "Neural network control of a class of nonlinear systems with actuator saturation," *IEEE Trans. Neural Netw.*, vol. 17, no. 1, pp. 147–156, Jan. 2006.

[25] O. Elhaki and K. Shojaei, "A robust neural network approximation-based prescribed performance output-feedback controller for autonomous underwater vehicles with actuators saturation," *Eng. Appl. Artif. Intell.*, vol. 88, Feb. 2020, Art. no. 103382, doi: 10.1016/j.engappai.2019.103382.

[26] M. Turner, J. Sofrony, and E. Prempain, "Anti-windup for model-reference adaptive control schemes with rate-limits," *Syst. Control Lett.*, vol. 137, Mar. 2020, Art. no. 104630, doi: 10.1016/j.sysconle.2020.104630.

[27] B. Rui, Y. Yang, and W. Wei, "Nonlinear backstepping tracking control for a vehicular electronic throttle with input saturation and external disturbance," *IEEE Access*, vol. 6, pp. 10878–10885, 2017, doi: 10.1109/ACCESS.2017.2783948.

[28] G. Ma, C. Chen, Y. Lyu, and Y. Guo, "Adaptive backstepping-based neural network control for hypersonic reentry vehicle with input constraints," *IEEE Access*, vol. 6, pp. 1954–1966, 2017.

[29] V. C. Pal and R. Negi, "Delay-dependent stability criterion for uncertain discrete time systems in presence of actuator saturation," *Trans. Inst. Meas. Control*, vol. 40, no. 6, pp. 1873–1891, Apr. 2018.

[30] H. Zhou, Y. Yang, H. Su, and W. Zeng, "Semi-global leader-following consensus of discrete-time linear multi-agent systems subject to actuator position and rate saturation," *Int. J. Robust Nonlinear Control*, vol. 27, no. 16, pp. 2921–2936, Nov. 2017.

[31] Y. Zhao, X. Sun, G. Wang, and Y. Fan, "Adaptive backstepping sliding mode tracking control for underactuated unmanned surface vehicle with disturbances and input saturation," *IEEE Access*, vol. 9, pp. 1304–1312, 2021.

[32] H. Luo, J. Yu, C. Lin, Z. Liu, L. Zhao, and Y. Ma, "Finite-time dynamic surface control for induction motors with input saturation in electric vehicle drive systems," *Neurocomputing*, vol. 369, pp. 166–175, Dec. 2019.

[33] B. Niu, H. Li, Z. Zhang, J. Li, T. Hayat, and F. E. Alsaadi, "Adaptive neural-network-based dynamic surface control for stochastic interconnected nonlinear nonstrict-feedback systems with dead zone," *IEEE Trans. Syst., Man, Cybern., Syst.*, vol. 49, no. 7, pp. 1386–1398, Jul. 2019.

[34] M. Chen, G. Tao, and B. Jiang, "Dynamic surface control using neural networks for a class of uncertain nonlinear systems with input saturation," *IEEE Trans. Neural Netw. Learn. Syst.*, vol. 26, no. 9, pp. 2086–2097, Sep. 2015.

[35] H. Niu, J. Yu, H. Yu, C. Lin, and L. Zhao, "Adaptive fuzzy output feedback and command filtering error compensation control for permanent magnet synchronous motors in electric vehicle drive systems," *J. Franklin Inst.*, vol. 354, no. 15, pp. 6610–6629, Oct. 2017.

[36] J. Yu, P. Shi, W. Dong, and H. Yu, "Observer and command-filter-based adaptive fuzzy output feedback control of uncertain nonlinear systems," *IEEE Trans. Ind. Electron.*, vol. 62, no. 9, pp. 5962–5970, Sep. 2015.

[37] J. A. Farrell, M. Polycarpou, M. Sharma, and W. Dong, "Command filtered backstepping," *IEEE Trans. Autom. Control*, vol. 54, no. 6, pp. 1391–1395, Jun. 2009.

[38] Y.-J. Liu, S. Tong, and C. L. P. Chen, "Adaptive fuzzy control via observer design for uncertain nonlinear systems with unmodeled dynamics," *IEEE Trans. Fuzzy Syst.*, vol. 21, no. 2, pp. 275–288, Apr. 2013.

[39] S. Yin, H. Gao, J. Qiu, and O. Kaynak, "Descriptor reduced-order sliding mode observers design for switched systems with sensor and actuator faults," *Automatica*, vol. 76, pp. 282–292, Feb. 2017.

[40] J. Zhang, X. Zhao, F. Zhu, and H. R. Karimi, "Reduced-order observer design for switched descriptor systems with unknown inputs," *IEEE Trans. Autom. Control*, vol. 65, no. 1, pp. 287–294, Jan. 2020.

YUMENG XU received the B.Sc. degree in electrical engineering and automation from Shandong Jiaotong University, Jinan, China, in 2019. She is currently pursuing the M.Sc. degree in control science and engineering with Qingdao University, Qingdao, China.

Her research interests include motor control, applied nonlinear control, and intelligent systems.

JIAPENG LIU received the M.Sc. degree in control science and engineering from Qingdao University, Qingdao, China, in 2015, and the Ph.D. degree in engineering from Shandong University, Jinan, China, in 2019.

He is currently a Distinguished Professor with the School of Automation, Qingdao University. His research interests include electrical energy conversion, ejector refrigeration, and model predictive control.

QIXIN LEI received the B.Sc. degree in automation from Qingdao University, Qingdao, China, in 2018, where he is currently pursuing the M.Sc. degree in control engineering.

His research interests include motor control, applied nonlinear control, and intelligent systems.

YUMEI MA received the B.Sc. degree in computer science and technology and the M.Sc. degree in computer application technology from Shandong University, Jinan, China, in 2002 and 2006, respectively, and the Ph.D. degree from the Institute of Complexity Science, Qingdao University, Qingdao, China, in 2014.

She is currently an Associate Professor with the College of Computer Science Technology, Qingdao University. Her research interests include nonlinear signal processing and weak signal detection.

JINPENG YU received the B.Sc. degree in automation from Qingdao University, Qingdao, China, in 2002, the M.Sc. degree in system engineering from Shandong University, Jinan, China, in 2006, and the Ph.D. degree from the Institute of Complexity Science, Qingdao University, in 2011.

He is currently a Distinguished Professor with the School of Automation, Qingdao University. His research interests include electrical energy conversion and motor control, applied nonlinear control, and intelligent systems. He was a recipient of Shandong Province Taishan Scholar Special Project Fund and Shandong Province Fund for Outstanding Young Scholars.

• • •